Multiresponsive Photopatterning Organic−Inorganic Polymer Hybrids Using a Caged Photoluminescence Compound

Tomoki Ogoshi, Junpei Miyake, and Yoshiki Chujo*

Department of Polymer Chemistry, Graduate School of Engineering, Kyoto University, Katsura, Nishikyo-ku, Kyoto 615-8510, Japan

Received December 25, 2004; Revised Manuscript Received March 15, 2005

ABSTRACT: The caged photoluminescence compound 2-(2′-benzoylphenyl)benzoxazole (BzPO) modified with poly(*N*,*N*-dimethylacrylamide) was synthesized. Transparent polymer hybrids with the obtained polymer were prepared by using hydrogen bond interactions between amide groups of the organic polymer and silanol groups resulting from hydrolysis of tetramethoxysilane. By UV irradiation upon the obtained polymer hybrids, the cage-released reaction of BzPO quickly took place even in a silica gel matrix, and the resulting polymer hybrids showed strong green photoluminescence deriving from a phototautomer of 2-(2′-hydroxyphenyl)benzoxazole (HPBO) dye. The preparation of "photoresist-like" photopatterning polymer hybrids could be also accomplished by using a photomask during UV irradiation. Furthermore, the photoluminescence of the polymer hybrids was reversibly quenched and emitted by the recaging of the hydroxyl group of HPBO with adsorption and desorption of water molecules. The miscibility of polymer hybrids depending on UV irradiation was evaluated by SEM and nitrogen adsorption porosimetry studies.

Introduction

The construction of hybrid materials by bridging organic and inorganic chemistries at the nanoscale or molecular scale has been an important field of current materials research in order to generate new advanced materials.[1−4] Organic polymer/inorganic hybrid materials have been elaborated with various inorganic hosts such as inorganic clay compounds,[5−7] metal oxo clusters,[8−10] mesoporous silica (zeolite),[11−13] and metallic or inorganic nanoparticles.[14−17] Among them, the sol−gel process employing metal alkoxides is an important and widely used technique for the preparation of organic−inorganic polymer hybrid materials.[18−25] Very convenient sol−gel access to inorganic solid under ambient conditions enables hybridization of organic polymer with inorganic oxides.[26] Silicon alkoxides such as tetramethoxysilane (TMOS) and tetraethoxysilane (TEOS) are mainly used as starting materials due to their mild sol−gel reactivity and easy handling. However, the poor compatibility between organic polymer and silica gel results in aggregation of organic polymer in a silica matrix during the formation of the silica gel, and then the appearance of the obtained composite materials is turbid or phase separated. To prepare homogeneous and transparent polymer hybrids, the improvement of the compatibility by introducing physical interaction or covalent bond between organic polymer and silica is necessary. Our group has elaborated novel transparent polymer hybrids by using physical interactions such as hydrogen bonding,[27−29] $\pi-\pi$ stacking,[30,31] and ionic[32] interactions between organic polymer and silica gel. For example, the formation of a hydrogen bond between organic polymers having hydrogen-accepting groups such as amide groups and hydrogen-donating groups of the residual silanol moieties resulted in the molecular dispersion of organic polymer in a silica gel matrix. The most striking property of the obtained polymer hybrids is optical transparency. Scattering loss is avoided due to nanoscale miscibility between organic polymer and silica.[33] Therefore, applications of these materials to optics have been desired and widely studied.

Scheme 1

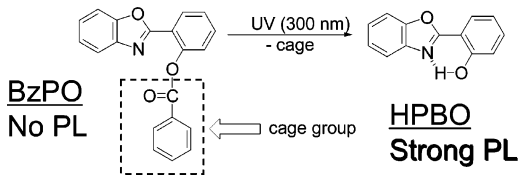

Recently, our group accomplished the construction of the photosensitive organic−inorganic polymer hybrid materials using a biological idea of caged (photoprotected) compounds.[34] Caged compounds are biologically inert molecules which can release bioactive compounds upon photolysis. The transparency of the obtained polymer hybrids could be controlled by introducing the caged compound into the interaction parts between organic polymer and siliceous phases. The UV irradiation resulted in the formation of the strong interaction between organic polymer and silica and the preparation of the highly transparent polymer hybrids, while the obtained materials without UV were turbid and phase separated.

Herein this research describes the other type of novel photosensitive organic−inorganic polymer hybrid materials utilizing a caged photoluminescent compound. Caged photoluminescent dyes usually show no photoluminescence (nonactive). However, upon photoirradiation, the cage moiety is released and the original photoluminescence is recovered (activated). Thus, caged photoluminescence compounds are mainly used for a biomedical indicator conjugated covalently with drugs.[35−38] Kocher et al. discovered that 2-(2′-benzoylphenyl)benzoxazole (BzPO), which exhibited no photoluminescence, was changed to a well-known PL compound of 2-(2′-hydroxyphenyl)benzoxazole (HPBO) by UV irradiation with a cleavage of the ether bond of BzPO (Scheme 1).[35]

The observation of no photoluminescence of BzPO derived from the inhibition of the intramolecular hy-

* Corresponding author: Tel +81-75-383-2604; Fax +81-75-383-2605; e-mail chujo@chujo.synchem.kyoto-u.ac.jp.

10.1021/ma047320d CCC: $30.25
Published on Web 04/15/2005

Scheme 2

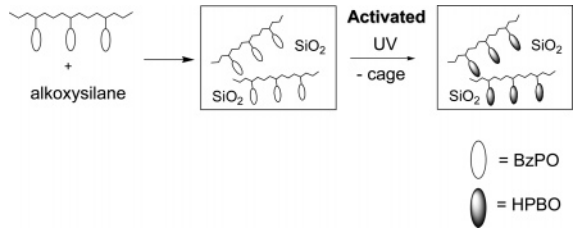

Scheme 3

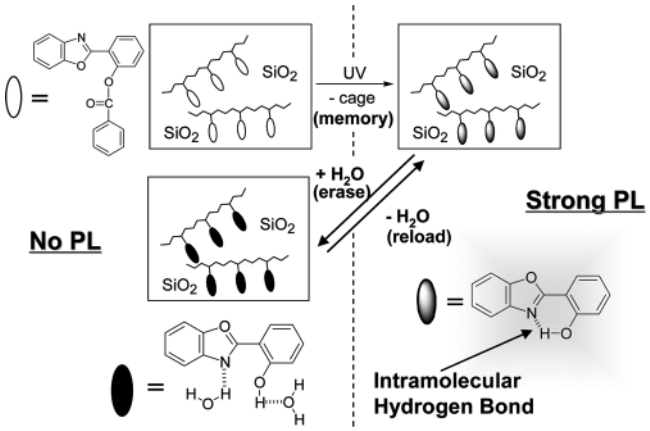

drogen bond between the nitrogen atom and hydroxyl group of HPBO. To show strong PL of HPBO, formation of the intramolecular hydrogen bond of HPBO is necessary.[39] The benzoic acid group of BzPO acted as a cage of the hydroxyl group of HPBO. In this study, the preparation of high transparent and homogeneous polymer hybrids with novel BzPO-modified polymer could be accomplished (Scheme 2). The obtained polymer hybrid showed strong photoluminescence with UV irradiation due to the generation of HPBO in a silica gel matrix. By using a photomask during UV irradiation, the synthesis of the photoresist-like polymer hybrids, which showed strong photoluminescence within UV-irradiated parts, could also be succeeded. Furthermore, the photoluminescence of the polymer hybrid was reversibly quenched and recovered by adsorption and desorption of water molecules (Scheme 3). Thus, the obtained polymer hybrid materials can memorize data by UV irradiation and reversibly erase−reload by adsorption−desorption of water molecules. Therefore, they are promisingly applied for optical memory devices, humidity sensors, and resist materials. The advantages of hybridizing BzPO-modified polymer with silica gel at a nanometer level are as follows: (1) The obtained polymer hybrids are perfectly transparent, which easily makes it a good candidate for optics. (2) The high transparency of polymer hybrids is maintained after hard treatments such as UV irradiation and water adsorption−desorption processes because of the reinforcement of organic polymer with silica gel at a nanometer level. (3) The photodurability of the PL compound should also increase since the destruction of the PL compound with UV irradiation in air should be impeded by hard silica gel matrix. To our best knowledge, it is the first example that the biological concept of caged photoluminescence compounds is applied for nanocomposite materials science.

Experimental Section

Materials. Tetrahydrofuran (THF) was dried and distilled over sodium under nitrogen. *N*,*N*-Dimethylacrylamide was distilled under reduced pressure and stored under nitrogen. Phenyltrimethoxysilane (PhTMOS), tetramethoxysilane (TMOS), and methyltrimethoxysilane (MeTMOS) were distilled and stored under nitrogen. The other solvents and reagents were used as supplied.

Scheme 4

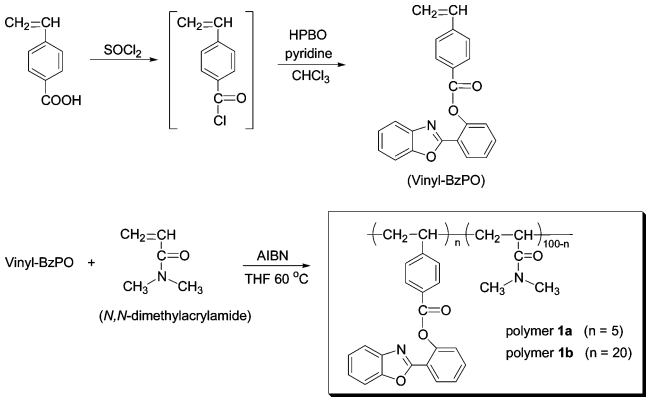

Measurements. The ^{1}H NMR spectra were recorded on a 400 MHz JEOL EX-400 spectrometer. Thermogravimetric analysis (TGA) was performed using a TG/DTA6200, SEIKO Instruments, Inc., with heating rate of 10 °C min^{-1} in air. Scanning electron microscopy (SEM) measurements were conducted using a JEOL JNM-5310/LV system. The FT-IR spectra were obtained using a Perkin-Elmer 1600 infrared spectrometer. Nitrogen adsorption porosimetry was conducted with a BEL Japan Inc. Fluorescence emission spectra were recorded on a Perkin-Elmer LS50B luminescence spectrometer. Gel permeation chromatography (GPC) analysis was carried out on TSK gel α-3000 by using DMF as an eluent at 40 °C after calibration with the standard polystyrene samples. Absorption spectra were obtained on a JASCO V-530 spectrometer.

Synthesis of 2-(2′-Benzoylphenyl)benzoxazole (Model Compound, BzPO). The model compound BzPO was prepared according to the detailed experimental procedure described in a previous literature.[35]

Synthesis of 2-(2′-*p*-Vinylbenzoylphenyl)benzoxazole (Vinyl-BzPO). Novel monomer having a BzPO moiety (vinyl-BzPO) was prepared as shown in Scheme 4.

Thionyl chloride ($SOCl_2$) (10.3 mL, 140 mmol) was added to *p*-vinylbenzoic acid (5.00 g, 33.9 mmol) at 0 °C under a nitrogen atmosphere. The temperature of the mixture was allowed to rise at room temperature, and the reaction mixture was stirred for 4 h. Then, the reaction mixture was stirred at 40 °C for 1 h to proceed the reaction completely. Excess thionyl chloride was evaporated under reduced pressure at 40 °C for 2 h. To the residual mixture, a solution of 2-(2′-hydroxyphenyl)-benzoxazole (HPBO, 4.49 g, 21.3 mmol) in 80 mL of chloroform was added at 0 °C. Then, 5.25 mL (15.8 mmol) of solution of pyridine was carefully added dropwise using a syringe at 0 °C, and the mixture was stirred at 0 °C for 1 h. Then, the reaction mixture was heated at 40 °C for 20 h. The resulting mixture was washed with water several times to remove pyridine HCl salt. The organic portion was dried over $MgSO_4$. The resulting solution was concentrated by evaporation and dried under reduced pressure. After the residual solid was recrystallized several times with methanol, a slightly yellow solid was obtained (vinyl-BzPO; 1.15 g, 3.36 mmol, yield 40.0%). ^{1}H NMR ($CDCl_3$): δ = 8.38 (m, 1H, BzPO), 8.25 (m, 2H, BzPO) 7.60−7.55 (m, 6H, BzPO), 7.39 (m, 2H, BzPO), 7.29 (m, 1H, BzPO), 6.87 (q, 1H, vinyl), 5.97 (d, 1H, vinyl), 5.47 (d, 1H, vinyl). IR (KBr, cm^{-1}): 1738 cm^{-1} (the stretching band of ester-carbonyl group), 1635 cm^{-1} (the stretching band of amide-carbonyl group). UV/vis ($CHCl_3$): 294 nm.

Synthesis of BzPO-Modified Poly(*N*,*N*-dimethylacrylamide) (Polymers 1a and 1b). Vinyl-BzPO/*N*,*N*-dimethylacrylamide copolymers were synthesized by a conventional free radical polymerization with changing the ratio of *N*,*N*-dimethylacrylamide to vinyl-BzPO (Scheme 4). A typical

preparation procedure for 5 mol % BzPO-modified poly(*N*,*N*-dimethylacrylamide) (polymer **1a**) is as follows. *N*,*N*-Dimethylacrylamide (0.706 mL, 6.87 mmol), vinyl-BzPO (0.295 g, 0.865 mmol), and AIBN (0.0280 g, 0.01 equiv molar ratio to monomer) were dissolved in 15 mL of THF solution under a nitrogen atmosphere. The mixture was refluxed for 24 h. The resulting solution was poured into hexane. The white solid was obtained (polymer **1a**: 1.81 g, yield 93.9%). ^{1}H NMR ($CDCl_3$): δ = 8.43−8.10 (m, BzPO), 7.60−7.00 (m, BzPO), 3.11−2.20 (m, N−C(CH_3)$_2$), 2.00−1.10 (m, Ar−CHCH_2 and −OCOCHCH_2). IR (KBr, cm^{-1}): 1740 cm^{-1} (the stretching band of ester−carbonyl group), 1635 cm^{-1} (the stretching band of amide−carbonyl group).

Preparation of Organic−Inorganic Polymer Hybrids. A typical preparation method of polymer hybrids using obtained polymers is as follows. The synthesized polymer was dissolved in a solvent. To the mixture, a solution of alkoxysilane and 0.1 or 1 M aqueous hydrochloric acid (as a catalyst for sol−gel reaction) was added. The resulting mixture was stirred at room temperature for certain time in a sealed bottle. Then, the resulting mixture was placed in a container covered with a paper towel and kept at 60 °C to evaporate the solvent. After evaporating the solvent completely, the polymer hybrids were obtained as a glassy material.

Photoinduced Cage-Released Reaction. The cage-released reaction of BzPO was induced by the irradiation of UV light using 175 W Xe lamp filtered with a Toshiba UV-D33S glass filter. The cage-released reaction was monitored by UV and PL spectra during photoirradiation of the polymer hybrids. Efficiencies of the cage-released reaction of the polymer hybrids were calculated by UV absorption at 332 nm by utilizing molar absorption coefficients of model compounds of BzPO and HPBO. Molar absorption coefficients of BzPO and HPBO at 332 nm were 1500 and 15 700 M^{-1} cm^{-1}, respectively.

Reversible Quenching and Recovering of Photoluminescence of Polymer Hybrids. To quench the photoluminescence of the polymer hybrids after UV irradiation, which showed strong photoluminescence of HPBO moieties due to removal of the cage groups by UV irradiation, the samples were left in a closed desiccator containing the solvent (water, methanol, and chloroform). Furthermore, after quenching the photoluminescence of the polymer hybrids, the hybrid materials were kept at 60 °C to remove the adsorbed solvent. The photoluminescence of the polymer hybrids depending on the processes of adsorption and desorption of the solvent was monitored by fluorescence emission measurement.

Nitrogen Adsorption Porosimetry. The powder of the polymer hybrid was heated at 600 °C in an ambient atmosphere for 24 h to remove organic polymer. The samples dried at 200 °C for 2 h at reduced pressure before porosimetry measurements. The surface area and pore volume were calculated by the Brunauer−Emmet−Teller (BET)[40] equation in the range of 0.05−0.30 (p/p_0), and the pore size distribution was estimated by the Barrett−Joyner−Halenda (BJH) method.[41]

Results and Discussion

Synthesis of BzPO-Modified Poly(*N*,*N*-dimethylacrylamide) (Polymers 1a and 1b). The novel BzPO monomer (vinyl-BzPO) was synthesized as illustrated in Scheme 4. The structure was characterized by ^{1}H NMR, UV, and FT-IR. BzPO-modified poly(*N*,*N*-dimethylacrylamide) was prepared with vinyl-BzPO and *N*,*N*-dimethylacrylamide monomer by free radical polymerization. Figure 1 shows the ^{1}H NMR spectrum of polymer **1a**, which has 5 mol % of BzPO groups at the PDMAAm polymer side chain. After radical polymerization, the vinyl peaks (5.00−6.90 ppm) from vinyl-BzPO and *N*,*N*-dimethylacrylamide disappeared completely, and the new BzPO peaks were observed around 8.43−8.10 and 7.60−7.00 ppm. The adsorption maximum of the polymers **1a** and **1b** was shown at 294 nm in chloroform, which was identified to that of BzPO group. (The molar absorption coefficient of BzPO at 294 nm was 19 600 M^{-1} cm^{-1}.) The introduction efficiency of BzPO moieties was calculated by ^{1}H NMR and UV measurements (Table 1). The introduction efficiency of BzPO in both polymers **1a** and **1b** was slightly small compared with the feed ratio, but BzPO moieties were successfully modified with polymer side chain. The obtained polymers should not be block but quite random polymers due to the alternating reactivity between vinyl-BzPO and styrene.

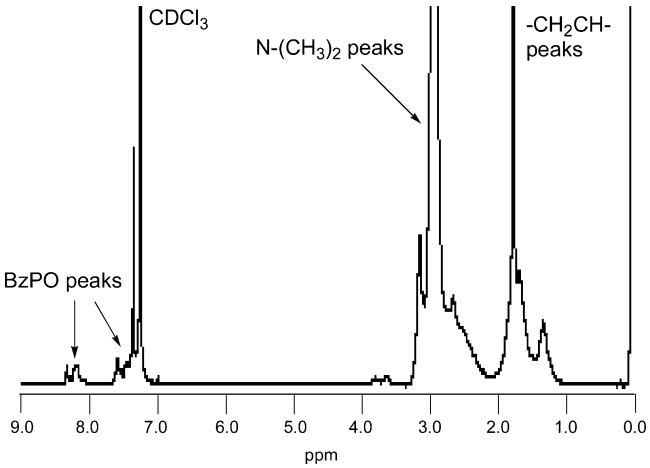

Figure 1. ^{1}H NMR spectrum of polymer **1a** (in $CDCl_3$).

Table 1. Synthesis of BzPO-Modified Poly(*N*,*N*-dimethylacrylamide) (Polymers 1a and 1b)

polymer	feed ratio (mol %)	degree of BzPO (mol %) UV	degree of BzPO (mol %) ^{1}H NMR	M_n	M_w/M_n	yield (%)
1a	5	4.5	3.6	4600	3.1	94
1b	20	15	17	6800	2.7	90

Synthesis of Organic−Inorganic Polymer Hybrids. Organic−inorganic polymer hybrids with the polymers **1a** and **1b** were prepared (Table 2). The obtained polymer hybrids using the polymer **1b** and TMOS brought about phase separation (runs 1−3). On the other hand, transparent polymer hybrids with the polymer **1a** were prepared (runs 4−6). These results are different from the previous study with poly(*N*,*N*-dimethylacrylamide), which is dispersed in a silica gel matrix at a nanometer level in a wide range without any difficulties due to the strong hydrogen bond between amide groups of poly(*N*,*N*-dimethylacrylamide) and residual silanol moieties of silica. The hydrogen bonds between poly(*N*,*N*-dimethylacrylamide) and silanol moieties from sol−gel reaction of tetramethoxysilane (TMOS) were confirmed by FT-IR measurement in previous papers.[27−29] The amide−carbonyl stretching band of poly(*N*,*N*-dimethylacrylamide) at 1638 cm^{-1} was shifted to 1625 cm^{-1} on hybridization with silica gel from TMOS, which is strong evidence of the hydrogen bonds. Therefore, it is considered that the modification of the BzPO moiety at the side chain of poly(*N*,*N*-dimethylacrylamide) largely effects the transparency of the obtained polymer hybrids. The BzPO moiety has a rather poor miscibility in the reaction mixture and high crystallinity; thus, BzPO groups tend to aggregate during the formation of the polymer hybrids. The polymer **1b** was modified with high molar percentages of BzPO moiety (20 mol %) compared to the polymer **1a** (5 mol %) so that the polymer hybrids using the polymer **1b** easily form aggregation of BzPO moieties and

Table 2. Synthesis of Organic–Inorganic Polymer Hybrids with Polymers 1a and 1b[a]

							ceramic yield (wt %)	
run	polymer (mg)	TMOS (mg)	ratio[b]	solvent (mL)	HCl_{aq}[c] (mL)	appearance	calcd	obsd[d]
1	**1b** 50	125	1	THF 2.5	0.1 M	phase separated		
2	**1b** 50	250	2	THF 2.5	0.1 M	phase separated		
3	**1b** 50	500	4	THF 5.0	0.1 M	phase separated		
4	**1a** 25	1000	16	MeOH 0.25	0.1 M	transparent	94.1	84.9
5	**1a** 25	500	8	MeOH 0.25	0.1 M	transparent	88.9	80.9
6	**1a** 25	250	4	MeOH 0.25	0.1 M	transparent	80.0	72.7
7	**1a** 50	250	2	MeOH 0.50	0.1 M	turbid		
8	**1a** 50	250	2	MeOH 0.50	1.0 M	transparent	66.7	60.2

[a] Stirring time was 1 h, and the solvent was evaporated at 60 °C. [b] Feed ratio of silica/polymer (w/w). [c] 4 equiv to TMOS. [d] Calculated by TGA.

Table 3. Synthesis of Organic–Inorganic Polymer Hybrids with Polymer 1b[a]

run	polymer **1b** (mg)	BzPO (mg)	PDMAAm[b] (mg)	$RSi(OMe_3)_3$	ratio[c]	appearance
9	25			Ph	16	transparent
10	25			OMe	16	turbid
11	25			Me	16	turbid
12	25			Ph	8	transparent
13	25			Ph	4	transparent
14	25			Ph	2	transparent
15	25			Ph	1	transparent
16		8	17	Ph	1	phase separated
17		8		Ph		phase separated

[a] 2.0 mL of THF was used as a solvent. The amount of 0.1 M HCl(aq) used was 4 equiv to TMOS and 3 equiv to MeTMOS and PhTMOS. Stirring time was 1 h, and the solvent was evaporated at 60 °C. [b] Poly(*N*,*N*-dimethylacrylamide). [c] Feed ratio of silica/polymer (w/w).

become phase separation. And with 1 M aqueous hydrochloric acid, transparent polymer hybrids using polymer **1a** content as mush as 33% could be obtained (runs 7 and 8). These observations mean that the problem of aggregation of BzPO moieties in the case of polymer **1a** could be overcome by controlling the acid concentration. Formation of siliceous oligomers is accelerated at high acid concentration.[26] That is, the gelation of TMOS using 1 M aqueous acid catalyst takes place faster than that using 0.1 M aqueous acid. Therefore, this fast reaction allows the reaction mixture to be frozen before the microscopic phase separation derived from aggregation of BzPO moieties and gives transparent polymer hybrids. The same trend was observed in the case of the preparation of polymer hybrids using poly(2-methyl-2-oxazoline) having functional groups.[43,44] The ceramic yields calculated by TGA measurement were slightly small compared with the theoretical ceramic yield because the small amounts of TMOS were evaporated before gelation of TMOS.

The high homogeneous polymer hybrids with polymer **1b** could be accomplished by using alkoxysilane having organic residues (Table 3). In the case of the samples using polymer **1b** and phenyltrimethoxysilane (PhTMOS), the obtained polymer hybrids were transparent in a wide range (runs 9 and 12–15). On the other hand, the appearance of the polymer hybrids using TMOS (run 10) or methyltrimethoxysilane (MeTMOS; run 11) was turbid. These observations strongly indicate that strong $\pi-\pi$ interaction between BzPO moieties of polymer **1b** and phenyl groups of PhTMOS efficiently inhibited the aggregation of BzPO groups during the preparation of the polymer hybrids. In the samples using BzPO (model compound) with PDMAAm (run 16) or without PDMAAm (run 17), the obtained materials showed phase separation. The preparation of high transparent polymer hybrids having BzPO moieties could be only achieved by introducing BzPO moieties into the polymer side chain. It is because the physical entrapment of the polymer chain by silica matrix deters BzPO aggregations.

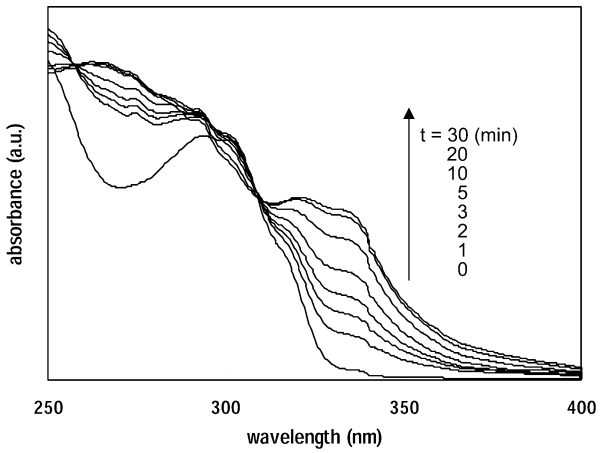

Figure 2. Changes of UV absorption of polymer **1a** during photoirradiation (in $CHCl_3$).

Photoinduced Cage-Released Reaction of Polymer Hybrids. The cage-released reaction of polymers **1a** and **1b** in solution was monitored by UV measurement. Figure 2 shows the change of UV absorption of polymer **1a** upon photoirradiation. The UV absorption peak at 332 nm derived from HPBO moieties gradually increased, indicating the progress of the cage-released reaction of BzPO moieties of polymer **1a**. Photoinduced cage-released reaction in a silica gel matrix was monitored by UV and PL measurements (Figure 3). The films of the polymer hybrid with polymer **1a** or **1b** were prepared on the quartz substrates. The changes of UV absorption and photoluminescence intensity during photoirradiation were checked. As shown in Figure 3a, the absorbance around 332 nm, which resulted from HPBO absorption, increased depending on the time of UV irradiation. The photoluminescence intensity around 500 nm was also increasing by UV irradiation (Figure 3b). From these observations, the cage-released reaction of the BzPO moiety in a silica gel matrix could be clearly confirmed.

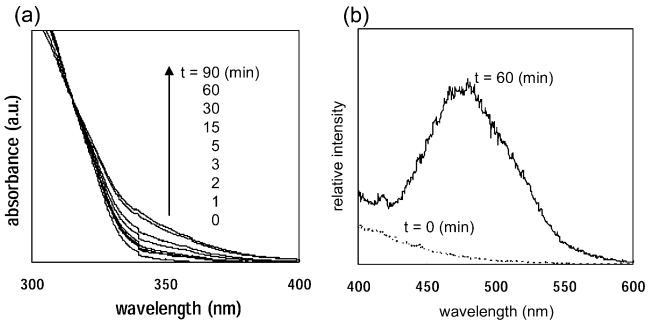

Figure 3. (a) UV and (b) PL spectra of the polymer hybrid film (run 6) during photoirradiation.

Table 4. Efficiency of Cage-Released Reaction of BzPO

run	polymer	$RSi(OMe)_3$	ratio[a]	appearance	efficiency (%)
4	**1a**	OMe	16	transparent	16.2
5	**1a**	OMe	8	transparent	10.1
6	**1a**	OMe	4	transparent	7.5
8	**1a**	OMe	2	transparent	8.2
12	**2a**	Ph	8	transparent	15.5
14	**2a**	Ph	2	transparent	21.0
polymer **1a** (in $CHCl_3$ solution)					84.9
polymer **2a** (in $CHCl_3$ solution)					66.8

[a] Feed ratio of silica/polymer (w/w).

The efficiencies of the cage-released reaction were calculated (Table 4). In the case of the polymer hybrids, the efficiencies were about 10–20%. In contrast, the cage-released reaction of polymers **1a** and **1b** efficiently proceeded in solution. The efficiencies of the cage-released reaction of polymers **1a** and **1b** in chloroform were 84.9% and 66.8%, respectively. As previously reported, the cage-released reaction of the model compound (BzPO) took place completely.[35] These observations result from the mechanism of the cage-released reaction. The UV irradiation leads to homolytic cleavage of the O–C(O) bond of BzPO moieties, yielding an HPBO and a benzoyl radical groups. Therefore, the recombination of both radical pairs should affect the cage-released efficiency. The recombination of radical pairs between HPBO and benzoyl radical moieties more easily occurred by incorporating the BzPO moieties into the polymer chain due to the steric hindrance. Furthermore, the recombination of radical pairs should more easily proceed in the silica gel because of the poor mobility of the radical pairs in hard silica gel matrix.

The photoluminescence of HPBO generated from the cage-released reaction of BzPO was also measured (Figure 4). As previously reported, the color of photoluminescence of HPBO dye largely depended on the environment;[39] HPBO had the ability to undergo an excited-state intramolecular proton transfer (ESIPT). Upon photoirradiation, the hydroxyl proton of HPBO is transferred to the adjacent nitrogen atom (ESIPT), and a "phototautomer" is generated as a result. The phototautomer of HPBO shows strong green photoluminescence at 490 nm. In nonpolar solvents such as chloroform and THF, the formation of the phototautomer of HPBO formed efficiently. The green strong emission of HPBO (Figure 4b; λ_{em} = 490 nm) was observed in chloroform. On the other hand, in polar solvents such as water and methanol, HPBO can form an intermolecular hydrogen bond with the solvent, which leads to inhibition of the ESIPT and shows normal blue PL of HPBO. HPBO showed an intense blue emission (Figure 4a; λ_{em} = 430 nm) in methanol. The

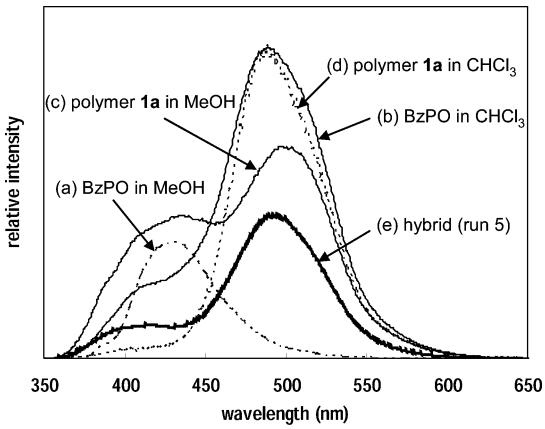

Figure 4. PL spectra of (a) BzPO in methanol, (b) BzPO in chloroform, (c) polymer **1a** in methanol, (d) polymer **1a** in chloroform, and (e) the polymer hybrid film (run 5) (excitation at 350 nm). All samples were measured after UV irradiation for 30 min.

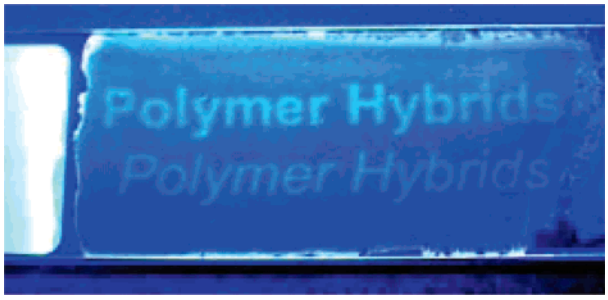

Figure 5. Picture of the transparent hybrid film (run 8) after UV (300 nm) irradiation with photomask.

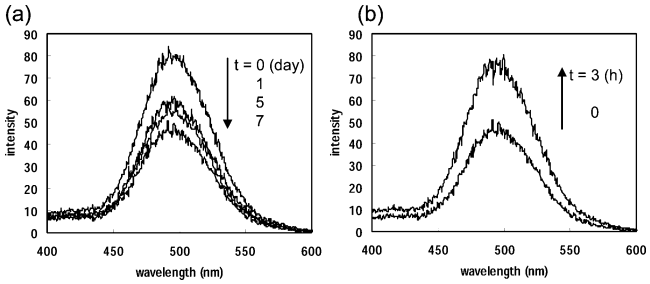

Figure 6. Changes of PL intensity of (a) the polymer hybrid film (run 6) after UV irradiation in saturated vapor pressure of water and (b) the polymer hybrid film (run 6) after annealing at 60 °C.

trend was almost the same in the case of the polymer **1a**. The photoluminescence resulting from polymer **1a** after UV irradiation showed a peak around 430 nm in methanol (Figure 4c), while the green emission (λ_{em} = 490 nm) was observed in chloroform (Figure 4d). In the case of the polymer hybrid after cage-released reaction, the photoluminescence of HPBO in a silica gel matrix from TMOS was observed at 490 nm (Figure 4e). These observations indicate that the excited HPBO molecules with UV irradiation efficiently form the phototautomer of HPBO through ESIPT in a silica gel matrix.

Photoresist-like Photoluminescent Organic–Inorganic Polymer Hybrids. By using a photoresist mask, the photoresist like organic–inorganic polymer hybrid could be prepared. The UV light was irradiated upon the photoresist mask. After UV irradiation, the appearance of the polymer hybrid was not changed compared to that before UV irradiation. The part with UV irradiation was fully colorless and transparent.

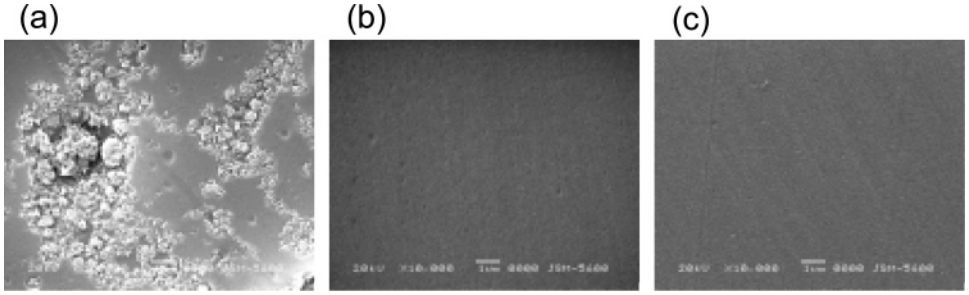

Figure 7. SEM images of (a) the phase-separated polymer hybrid (run 7), (b) the transparent polymer hybrid (run 8) before UV irradiation, and (c) the transparent polymer hybrid (run 8) after UV irradiation.

Scheme 5

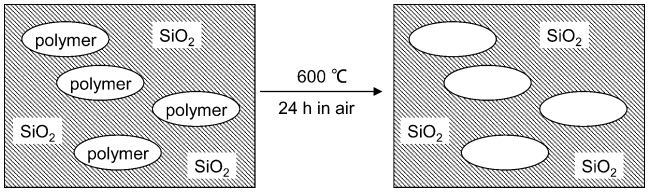

But, the part with photoirradiation showed strong green photoluminescence, and the characters "polymer hybrids" clearly appeared by excitation at 365 nm (Figure 5).

Reversible PL Properties of Organic−Inorganic Polymer Hybrids. The photoluminescence of HPBO was affected by the intramolecular hydrogen bond between the hydroxyl group and nitrogen atom of HPBO. The PL of HPBO was quenched by inhibition of the intramolecular hydrogen bond of HPBO. Therefore, the intensity of the photoluminescence of HPBO should be quenched and recovered by reversible formation of the intramolecular hydrogen bond of HPBO.[39] In this study, the photoluminescence of HPBO in a silica matrix was reversibly quenched and recovered by adsorption and desorption of water molecules into the polymer hybrid film after cage-released reaction of BzPO. At first, the changes of the intensity of the photoluminescence of HPBO in silica gel were monitored during the adsorption of water molecules. As shown in Figure 6a, the PL intensity at 490 nm of HPBO declined gradually with increasing of the keeping time under the saturated vapor pressure of water at 25 °C. In contrast, the quenching of the photoluminescence was not observed under the saturated vapor pressure of methanol and chloroform. These observations mean the formation of an intermolecular hydrogen bond between the water molecule and hydroxyl group of HPBO, as shown in Scheme 3. The intermolecular hydrogen bond between the water molecule and hydroxyl group of HPBO inhibited ESIPT and photoluminescence. Then, the sample was left in an oven at 60 °C. As shown in Figure 6b, the intensity of photoluminescence was recovered perfectly by keeping the hybrid at 60 °C, suggesting the removal of water molecules and re-formation of the intramolecular hydrogen bond between the nitrogen atom and hydroxyl group of HPBO.

SEM and Nitrogen Adsorption Studies To Investigate Homogeneity of Organic−Inorganic Polymer Hybrids. The miscibility between polymer **1a** and silica phases was examined by SEM and nitrogen adsorption porosimetry studies. Figure 7 showed SEM images of the obtained polymer hybrids with polymer **1a**. In the case of the turbid sample (Table 1, run 7), bright domains were clearly found at 10 000 magnifications (Figure 7a). White parts indicate silica phase. On the other hand, in the transparent polymer hybrid (Table 1, run 8), bright domains could not be observed even at 10 000 magnifications (Figure 7b). No (black) image in Figure 7b at 10 000 magnifications indicates high homogeneity of the transparent polymer hybrid compared with the turbid composite. The nanolevel dispersion of some hybrid materials showed the same results in the SEM as previously reported in our group.[30−32,34,45] The SEM image of the polymer hybrid was not changed after UV irradiation (Figure 7c). It means that the polymer hybrids keep high homogeneity with UV irradiation.

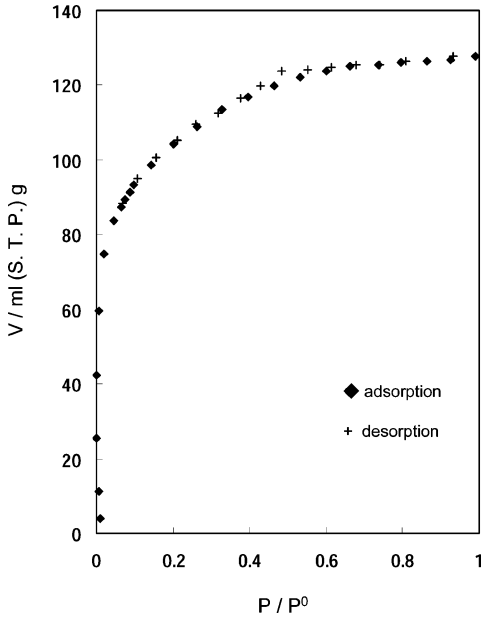

Figure 8. Adsorption isotherm curve of the transparent polymer hybrid (run 6) before UV irradiation.

The homogeneity of the polymer hybrids was also quantitatively evaluated on the nanometer scale by nitrogen adsorption porosimetry study. The porous silica was prepared by burning out the organic polymer of the polymer hybrids at 600 °C for 24 h (Scheme 5). The silica gel matrix is so rigid that the size of the pores obtained by calcination of the polymer hybrids is found to be the domain of the organic polymer. The previously reported paper actually confirmed that the size of the porous silica reflected the organic polymer domain. For example, the pore size of the porous silica prepared by calcination of the hybrids with dendrimer was almost the same as the size of the dendrimer used.[28] The pore size of the obtained porous silica became larger according to the increasing of the generation of the used dendrimer. The porous silica obtained by charring the

Table 5. Porosity of the Silica Obtained by Calcinating Polymer Hybrids

run	pore vol[a] (mL/g)	surf. area[a] (m^2/g)	pore radius[b] (nm)
6	117	119	1.1
6[c]	206	145	1.7

[a] Calculated by BET. [b] Calculated by the BJH method. [c] The porous silica obtained by calcination of the polymer hybrid (run 6) after UV irradiation.

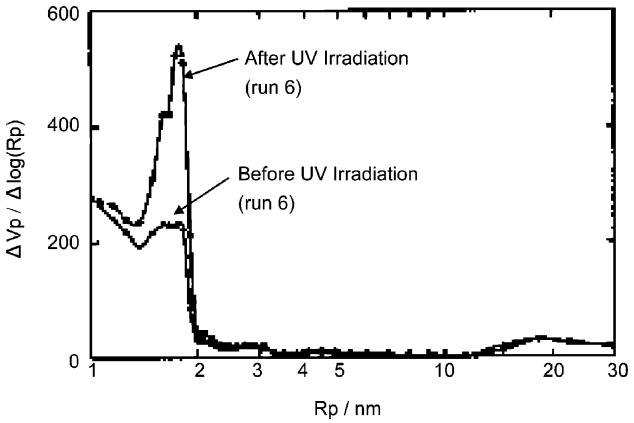

Figure 9. Pore size distribution plots of porous silica obtained from the transparent polymer hybrid (run 6) (a) before UV irradiation and (b) after UV irradiation.

cyclodextrin/silica hybrid was also equal to the cavity size of the cyclodextrin.[45]

The adsorption isotherm curve obtained by the nitrogen adsorption measurement of the porous silica from the polymer hybrid (run 6) is shown in Figure 8. The shape of the curve was a type IV curve, indicating that the porous silica had nanopores. The porous silica obtained by the polymer hybrid (run 6) after UV irradiation also gave the IV curve. The pore volume and the surface area of the porous silica were calculated by the BET method. Both porous silicas had large surface area and pore volume (Table 5). The pore size distribution of the porous silica was also calculated by the BJH method (Figure 9). The size of the pore was below 2.0 nm even if the polymer hybrid was subjected to UV irradiation. This result confirms the nanoscale miscibility of the polymer hybrid independent of the UV irradiation.

Conclusions

High transparent homogeneous polymer hybrids were obtained with novel BzPO-modified polymer. The cage-released reaction of BzPO upon UV irradiation proceeded in a silica gel matrix. The photopatterning polymer hybrids, which showed strong photoluminescence within UV irradiated area, were also prepared using a photomask during UV irradiation. The PL of the polymer hybrids was reversibly quenched and emitted by adsorption−desorption of water molecules. Thus, the obtained polymer hybrids can be applied for memory devices by writing data using UV light, erasing, and reloading data using adsorption−desorption of water molecules.

References and Notes

(1) Special issues for nanocomposite materials. *Chem. Mater.* **1996**, *8* (8); *Chem. Mater.* **1997**, *9* (11); *Chem. Mater.* **2001**, *13* (10); *MRS Bull.* **2001**, *26* (5).
(2) Schmid, G.; Maihack, V.; Lantermann, F.; Peschel, S. *J. Chem. Soc., Dalton Trans.* **1996**, 589.
(3) Beecroft, L. L.; Ober, C. K. *Chem. Mater.* **1998**, *10*, 1440.
(4) Sanchez, C.; Lebeau, B.; Chaput, F.; Boilot, J.-P. *Adv. Mater.* **2003**, *23*, 1969.
(5) Usuki, A.; Kawasumi, M.; Kojima, Y.; Fukushima, Y.; Okada, A.; Kurauchi, T.; Kamigaito, O. *J. Mater. Res.* **1993**, *8*, 1179.
(6) Usuki, A.; Hasegawa, N.; Kadoura, H.; Okamoto, T. *Nano Lett.* **2001**, *1*, 271.
(7) Okamoto, M.; Nam, P. H.; Maiti, P.; Kotaka, T.; Nakayama, T.; Takada, M.; Ohshima, M.; Usuki, A.; Hasegawa, N.; Okamoto, H. *Nano Lett.* **2001**, *1*, 503.
(8) Jousseaume, B.; Lahcini, M.; Rascle, M.-C.: Ribot, F.; Sanchez. C. *Organometallics* **1995**, *14*, 685.
(9) Trimmel, G.; Fratzl, P.; Schubert, U. *Chem. Mater.* **2000**, *12*, 602.
(10) Otero, T. F.; Cheng, S. A.; Huerta, F. *J. Phys. Chem. B* **2000**, *104*, 10522.
(11) Kageyama, K.; Tamazawa, J.; Aida, T. *Science* **1999**, *285*, 2113.
(12) Ji, X.; Hampsey, J. E.; Hu, Q.; He, J.; Yang, Z.; Lu, Y. *Chem. Mater.* **2003.** *15.* 3656.
(13) MacLachlan, M. J.; Ginzburg, M.; Coombs, N.; Raju, N. P.; Greedan, J. E.; Ozin, G. A.; Manners, I. *J. Am. Chem. Soc.* **2000**, *122*, 3878.
(14) Hirai, H.; Nakao, Y.; Toshima, N. *J. Macromol. Sci., Chem., Suppl.* **1985**, *14*, 55.
(15) Toshima, N.; Yonezawa, T. *New J. Chem.* **1998**, *22*, 1179.
(16) Zhou, Y.; Itoh, H.; Uemura, T.; Naka, K.; Chujo, Y. *Chem. Commun.* **2001**, 613.
(17) Naka, K.; Itoh, H.; Chujo, Y. *Nano Lett.* **2002**, *2*, 1183.
(18) Wen, J.; Wilkes, G. L. *Chem. Mater.* **1996**, *8*, 1667.
(19) Loym, D. A.; Shea, K. J. *Chem. Rev.* **1995**, *95*, 1431.
(20) Novak, B. M. *Adv. Mater.* **1993**, *5*, 422.
(21) Giannelis, E. P. *Adv. Mater.***1996**, *8*, 29.
(22) Chujo, Y.; Tamaki, R. *MRS Bull.* **2001**, *26*, 389.
(23) Ichinose, I.; Kunitake, T. *Chem. Rec.* **2002**, *2*, 339.
(24) Sanchez, C.; Ribot, F.; Lebeau, B. *J. Mater. Chem.* **1999**, *9*, 35.
(25) Moreau, J. J. E.; Man, M. W. C. *Coord. Chem. Rev.* **1998**, *178−180*, 1073.
(26) Brinker, C. J.; Scherer, G. W. *Sol−Gel Science, The Physics and Chemistry of Sol−Gel Processing*; Academic Press: San Diego, 1990.
(27) Chujo, Y.; Ihara, E.; Kure, S.; Saegusa, T. *Macromolecules* **1993**, *26*, 5681.
(28) Chujo, Y.; Matsuki, H.; Kure, S.; Saegusa, T.; Yazawa, T. *J. Chem. Soc., Chem. Commun.* **1994**, 635.
(29) Chujo, Y.; Saegusa, T. *Adv. Polym. Sci.* **1992**, *100*, 11.
(30) Tamaki, R.; Samura, K.; Chujo, Y. *Chem. Commun.* **1998**, 1131.
(31) Tamaki, R.; Han, S. Y.; Chujo, Y. *Polym. Prepr. Jpn.* **1998**, *47*, 1016.
(32) Tamaki, R.; Chujo, Y. *Chem. Mater.* **1995**, *7*, 1719.
(33) Bohren, C. F.; Huffman, D. R. *Absorption and Scattering of Light by Small Particles*; Wiley: New York, 1983.
(34) Ogoshi, T.; Chujo, Y. *Macromolecules* **2004**, *37*, 5916.
(35) Kocher, C.; Smith, P.; Weder, C. *J. Mater. Chem.* **2002**, *12*, 2620.
(36) Kim, J.-M.; Kang, J.-H.; Han, D.-K.; Lee, C.-W.; Ahn, K.-D. *Chem. Mater.* **1998**, *10*, 2332.
(37) Kim, J.-M.; Chang, T.-E.; Kang, J.-H.; Han, D.-K.; Ahn, K.-D. *Adv. Mater.* **1999**, *11*, 1499.
(38) Kim, J.-M.; Chang, T.-E.; Kang, J.-H.; Park, K. H.; Han, D.-K.; Ahn, K.-D. *Angew. Chem., Int. Ed.* **2000**, *39*, 1780.
(39) Das, K.; Sarkar, N.; Ghosh, A. K.; Majumdar, D.; Nath, D. N.; Bhattacharyya, K. *J. Phys. Chem.* **1994**, *98*, 9126.
(40) Brunauer, S.; Emmett, P. H.; Teller, E. *J. Am. Chem. Soc.* **1938**, *60*, 45.
(41) Barrett, E. P.; Joyner, L. G.; Halenda, P. P. *J. Am. Chem. Soc.* **1951**, *73*, 373.
(42) Saini, G.; Leoni, A.; Franco, S. *Makromol. Chem.* **1971**, *146*, 165.
(43) Imai, Y.; Naka, K.; Chujo, Y. *Polym. J.* **1998**, *30*, 990.
(44) Imai, Y.; Ogoshi, T.; Naka, K.; Chujo, Y. *Polym. Bull. (Berlin)* **2000**, *45*, 9.
(45) Ogoshi, T.; Chujo, Y. *Macromolecules* **2003**, *36*, 654.

MA047320D